

On the origin of diffuse clouds

Richard J. Price,¹ Serena Viti^{2*} and David A. Williams¹

¹*Department of Physics and Astronomy, University College London, Gower Street, London WC1E 6BT*

²*CNR-Istituto di Fisica dello Spazio Interplanetario, Area di Ricerca di Tor Vergata, via del Fosso del Cavaliere 100, I-00133, Roma, Italy*

Accepted 2003 May 1. Received 2003 April 10; in original form 2003 March 6

ABSTRACT

We explore the possibility that observational differences might exist between diffuse clouds which have been formed from the dissipation of unbound molecular clouds and those which have been formed from less dense atomic gas. Using single-point chemical models, we show that molecular-rich initial conditions will significantly enrich the gas-phase chemistry of diffuse clouds in the former scenario. An injection of hydrogenated grain mantles through photoevaporation will also enrich this chemistry further. If the population of interstellar diffuse clouds contains some members that are in contraction and others that are in expansion, then wide variations in atomic and molecular abundances are to be expected in this population. We predict several signatures of this effect.

Key words: ISM: abundances – ISM: clouds – ISM: molecules.

1 INTRODUCTION

Diffuse interstellar clouds are typically detected along relatively low-extinction (visual extinction $A_V < 1$ mag) lines of sight towards nearby bright stars in UV, and in visual absorption lines of atoms, atomic ions and several molecules (cf. van Dishoeck 1998). Two well-studied examples are the lines of sight towards ζ Per and ζ Oph, towards which the visual extinction is ≈ 0.9 mag in both cases. Each of these lines of sight shows a number of distinct Doppler components, assumed to be different regions of diffuse matter along the lines of sight. For the main components towards ζ Per and ζ Oph, respectively, the observational data suggest that the total hydrogen number densities are 100 and 300 cm^{-3} , with the temperatures in both components being about 30 K. Both components contain appreciable amounts of molecular hydrogen ($\text{H}_2/\text{H} = 0.75$ and 0.85, respectively). Of course, these values are line-of-sight averages; local conditions may vary widely. For example, there is considerable evidence for the existence of small-scale (≈ 10 au) structures in at least some diffuse clouds in which the densities may be around two orders of magnitude larger than those quoted above for ζ Per and ζ Oph (Price, Crawford & Barlow 2000; Hartquist, Falle & Williams 2003).

Nevertheless, taking the mean number density and an inferred linear dimension for a diffuse cloud, then – depending somewhat on the adopted geometry – diffuse clouds apparently contain a significant fraction of the total interstellar mass of the Galaxy (cf. Dyson & Williams 1997), possibly comparable to that of the denser molecular clouds that are the sites of star formation. Yet the role of diffuse clouds in the general circulation of matter into and out of clouds and stars has not been elucidated fully. It is possible that diffuse clouds

are simply the envelopes of dark clouds (Federman & Allen 1991). However, in this paper, we consider the role of diffuse clouds in a dynamically evolving interstellar medium. A conventional view is that diffuse clouds are accumulations of gas swept up from even more tenuous intercloud atomic gas by wind-blown bubbles around massive stars (Hollenbach, Chu & McCray 1976). In this picture, molecular absorptions along the line of sight through the diffuse cloud arise from molecules formed in a simple chemistry in the initially atomic gas. Since the material has low visual extinction, the chemistry is dominated by photoprocesses initiated by the mean interstellar radiation field; thus, diffuse clouds are canonical photon-dominated regions (PDRs). After appreciable H_2 has formed, diffuse cloud chemistry attains a steady state on the time-scale determined by the photodissociation time-scales; these are short – typically 10^3 – 10^4 yr. The formation of H_2 takes much longer, $\sim 10^6$ yr (Wagenblast 1992). Alternatively, one might consider diffuse clouds to be in a transient phase of a dynamic cycle of matter into and out of star-forming regions. The diffuse clouds envisaged by Hollenbach et al. as swept-up tenuous gas may accumulate into regions denser than typical diffuse clouds, i.e. into molecular clouds and star-forming regions. Therefore, in this picture, diffuse clouds would represent a transient phase during this contraction from tenuous to dense molecular gas. Once star formation occurs, the observational evidence of stellar winds, outflows, and explosions (cf. Goldsmith, Langer & Wilson 1986; Bachiller 1996) indicates that dense molecular gas is returned to a more tenuous form. Thus, diffuse clouds may also represent a transient phase in the expansion of dense gas into a more tenuous form. The relation between these possible origins in the concept of a dynamical interstellar medium is illustrated in Fig. 1.

Is it possible that both types of diffuse cloud illustrated in Fig. 1 exist? Are the contraction- and expansion-phase diffuse clouds

*E-mail: viti@sirius.ifs1.rm.cnr.it

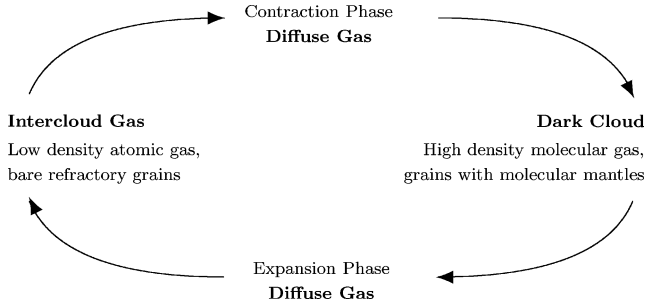


Figure 1. Diffuse clouds may be considered to be a transient phase in a cyclical interstellar process.

observationally distinguishable? If so, then we could learn something about the dynamical cycle of interstellar matter. To explore these questions, we report in this paper the results of a simple study of interstellar diffuse cloud chemistry, in both collapse and expansion phases. We do not consider here the static model, as this has been the conventional picture in most diffuse cloud studies to date (cf. Wagenblast & Williams 1993). The chemical and physical models we use are described in Section 2; the results are presented in Section 3, and Section 4 gives a brief discussion of the implications of these results.

2 THE MODEL

2.1 Chemistry

We adopt a conventional gas-phase chemistry from the UMIST data base (Millar, Farquhar & Willacy 1997). The H_2 formation rate (gr) is related to the gas temperature by the following equation:

$$gr = 1.0 \times 10^{-17} \sqrt{T} \text{ cm}^3 \text{ s}^{-1}. \quad (1)$$

H_2 is destroyed by absorption in the Lyman and Werner bands. We use the formulation of van Dishoeck & Black (1988) and Wagenblast (1992) for the photodissociation of CO and of H_2 , which is also destroyed by a line absorption process. There are 4346 gas-phase reactions representing the chemistry of 491 species in the adopted chemical network. In addition, because H_2O ice is observed to be abundant in denser gas, and because this molecule cannot be made in sufficient abundance in the gas phase (Jones & Williams 1984; O’neill & Williams 1999), we include the hydrogenation of atoms at the surfaces of dust grains in our network. Molecules in the ices are assumed to be returned to the gas through photodesorption, using the relatively low photon efficiency determined by Westley et al. (1995) for cometary ices in the Solar system. In the unshielded situation, this yields a photodesorption flux of simple hydrides into the gas phase of the order of 10^4 molecule $\text{cm}^{-2} \text{ s}^{-1}$; this allows the injection to continue for time-scales of more than 1 Myr.

The adopted initial elemental abundances are shown in Table 1. A discussion of the sensitivity of the chemistry to changes in these parameters is given in Section 3.

The chemical rate equations are integrated in time from initial conditions that are purely atomic, in a collapse that leads to high-density gas. It is then assumed that the density remains constant while the chemistry evolves for a further million years. This high-density gas is then taken as the starting point for the expansion phase. The results are computed at a single point, for which the density, temperature and A_V are determined by the physical models adopted for the collapse and expansion.

Table 1. Elemental abundances assumed in models.

Element	Abundance
H	1.0
He	1.4×10^{-1}
C	2.2×10^{-4}
O	4.6×10^{-4}
N	6.0×10^{-5}
S	1.3×10^{-5}
Na	2.0×10^{-7}
Si	7.0×10^{-9}
Mg	7.0×10^{-9}
Cl	2.0×10^{-9}
Fe	2.0×10^{-9}
P	1.0×10^{-9}

2.2 Physics

The contraction phase is modelled as a ‘modified free-fall’ collapse (Spitzer 1978; Nejad, Williams & Charnley 1990; Rawlings et al. 1992); in this model, the number density of hydrogen nuclei, n varies from the initial value, n_o , as

$$dn/dt = B \left(n^4 / n_o \right)^{1/3} \left\{ 24\pi G m_H n_o \left[(n/n_o)^{1/3} - 1 \right] \right\}^{1/2}. \quad (2)$$

Here, $B = 1$ represents free-fall; for $B < 1$, the collapse is slower than free-fall. Retarded collapse may occur if thermal or magnetic pressure is significant.

The radiation field and the cosmic ray ionization rate (ζ) employed are the standard interstellar medium UV field as determined by Habing (1968), and $1.3 \times 10^{-17} \text{ s}^{-1}$, respectively.

The visual extinction associated with the sample point is linked to number density, n , in the following manner:

$$A_V = 0.42 \times \log(n) - 0.867. \quad (3)$$

Equation (3) is merely a curve fit which relates plausible A_V and number density values. The constants in equation (3) are chosen so that the initial (10 cm^{-3}) and final (10^4 cm^{-3}) states correspond to visual extinctions of 0.1 and 3.0 magnitudes, respectively. A visual extinction of 1.0 magnitude is reached at a density of $\sim 100 \text{ cm}^{-3}$. We use the A_V generated from this equation directly in the photochemical rates, as listed in the UMIST data base (Millar et al. 1997). It may be that this value is an overestimate, because a ‘cloud’ represented by a single point may only be shielded by half of this A_V ; if so, then the computed abundances may be slightly too large. During the collapse, the temperature of the gas is decreased from 1000 K to 10 K, passing through 100 K at a density of $\sim 100 \text{ cm}^{-3}$.

We assume that the expansion of an overpressured parcel of gas after ejection by star formation processes in a dense molecular cloud is limited by the sound speed, c_0 . This is an overestimate, because the ambient gas around the parcel exerts a constraining pressure. Because magnetic fields are likely to restrict expansion in one dimension, a two-dimensional expansion of a parcel of size L_0 gives a number density evolution of

$$n = n_o / [1 + (\alpha t / t_0)]^2, \quad (4)$$

where $t_0 = L_0 / c_0$. For a three-dimensional expansion, the exponent would be 3. Here, α is a parameter which may be adjusted in order to vary the time required to reach diffuse cloud densities. The value adopted here – after several trials – was 0.2. For plausible choices of L_0 and the initial state of the parcel, equation (4) shows that number

densities comparable with those of diffuse clouds are obtained after evolutionary times of ≈ 1 Myr.

The visual extinction during the expansion phase is governed in the same manner as described for the collapse, but in the opposite sense.

3 CALCULATIONS AND RESULTS

Figs 2 and 3 illustrate the fractional abundances of a number of species over time in the collapse and expansion phases, respectively.

During the collapse phase, densities of 100 and 300 cm^{-3} are reached after periods of 1.4×10^7 and 1.5×10^7 yr, respectively. In the case of the expansion phase, densities of 300 and 100 cm^{-3} are reached after periods of 7.6×10^5 and 1.4×10^6 yr of expansion, respectively.

During the collapse phase, the molecular hydrogen fraction rises from being at a nearly atomic state at $t = 0$ (10 cm^{-3}) to become equal with the atomic hydrogen fraction by about 7×10^6 yr. The molecular hydrogen fraction continues to rise throughout the simulation, with the atomic hydrogen fraction falling off more rapidly as density increases. Once a density of 10^4 cm^{-3} is reached (~ 16 Myr), hydrogen is all in molecular form.

Of course, during the expansion phase, the atomic hydrogen fraction rises steadily with the falling density, until almost all hydrogen is again in atomic form when we reach a density of 10 cm^{-3} .

Before a reasonably high density is achieved, the curves of Figs 2 and 3 are shaped by the change in the dominant formation routes: at the lower densities, radiative association with H atoms is important. As H declines, so do the products of this chemistry. At higher densities, the chemistry is dominated instead by reactions with molecular hydrogen and so, as the density rises, the formation rates rise as

well. During contraction, when the density is high enough ($\sim 5 \times 10^3 \text{ cm}^{-3}$), depletion on to grains becomes important, yielding a decrease in the abundances of gas-phase species.

Theoretical column density estimates may be derived from these abundances and compared with observations, as collected by O’neill, Viti & Williams (2002). Focusing on spatial densities of 100 and 300 cm^{-3} , we can compare our models with observations of ζ Per (for 100 cm^{-3} ; see Table 2) and ζ Oph (for 300 cm^{-3} ; see Table 3). Although the results computed for densities of 100 and 300 cm^{-3} are not intended to model directly the clouds in the lines of sight to ζ Per and ζ Oph, they do illustrate that plausible diffuse cloud models can be achieved in the expansion and contraction scenarios. Note, however, that the theoretical estimates of column densities obtained from these single-point models are necessarily crude, and to attempt a more detailed comparison using accurately determined column densities, one would need to carry out a complete time and space description of the collapse and expansion mode chemistries. Such a calculation is beyond the scope of the present study.

Observed column densities enclosed in brackets in Tables 2 and 3 are for observations of lines of sight other than those towards ζ Per and ζ Oph, respectively. In these situations, the total hydrogen column densities may not be the same as those with which the comparison is being made. The CS column density listed in Table 2 and the SO column density listed in Tables 2 and 3 represent observations towards extragalactic millimetre radio sources, where the spatial density is expected to be approximately a few hundred cm^{-3} (Lucas & Liszt 1997). In the case of the observed column densities of C_2H and C_3H_2 in Tables 2 and 3, Lucas & Liszt (2000) imply spatial densities of approximately a few hundred cm^{-3} again. The column density of H_3^+ in Table 2 is taken from recent observations by McCall et al. (2003). They find a surprisingly large column density.

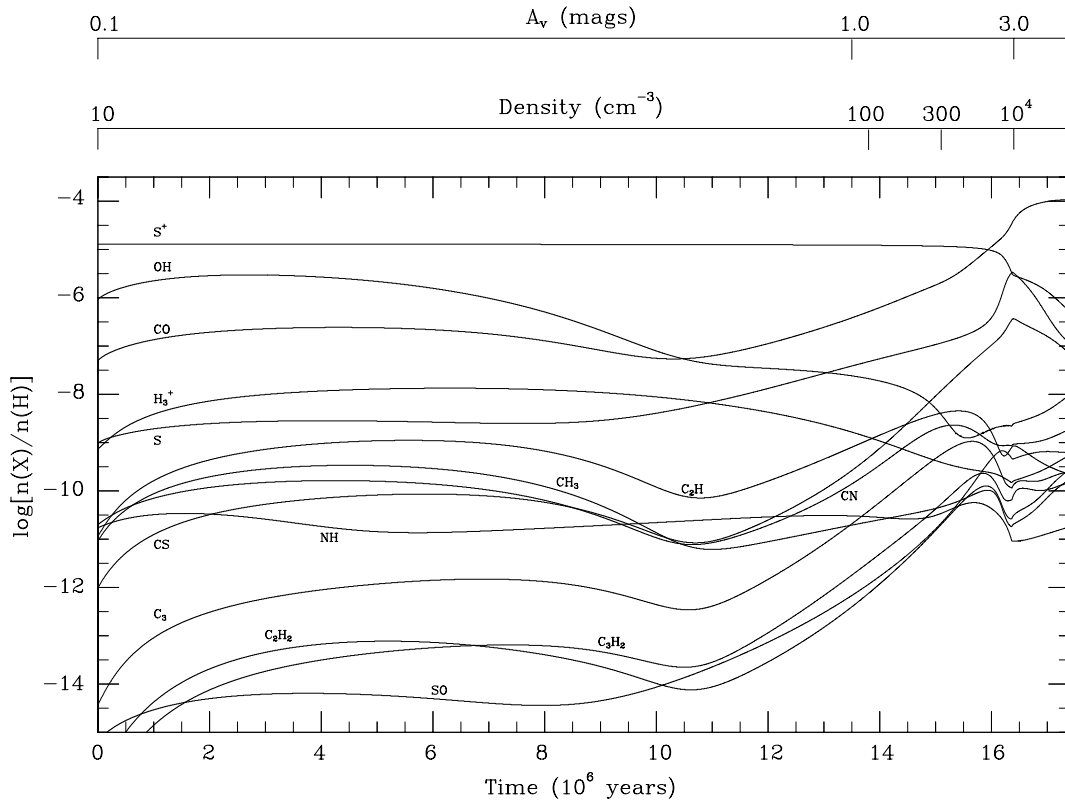


Figure 2. The fractional abundance of a selection of species relative to hydrogen over time, during the collapse phase.

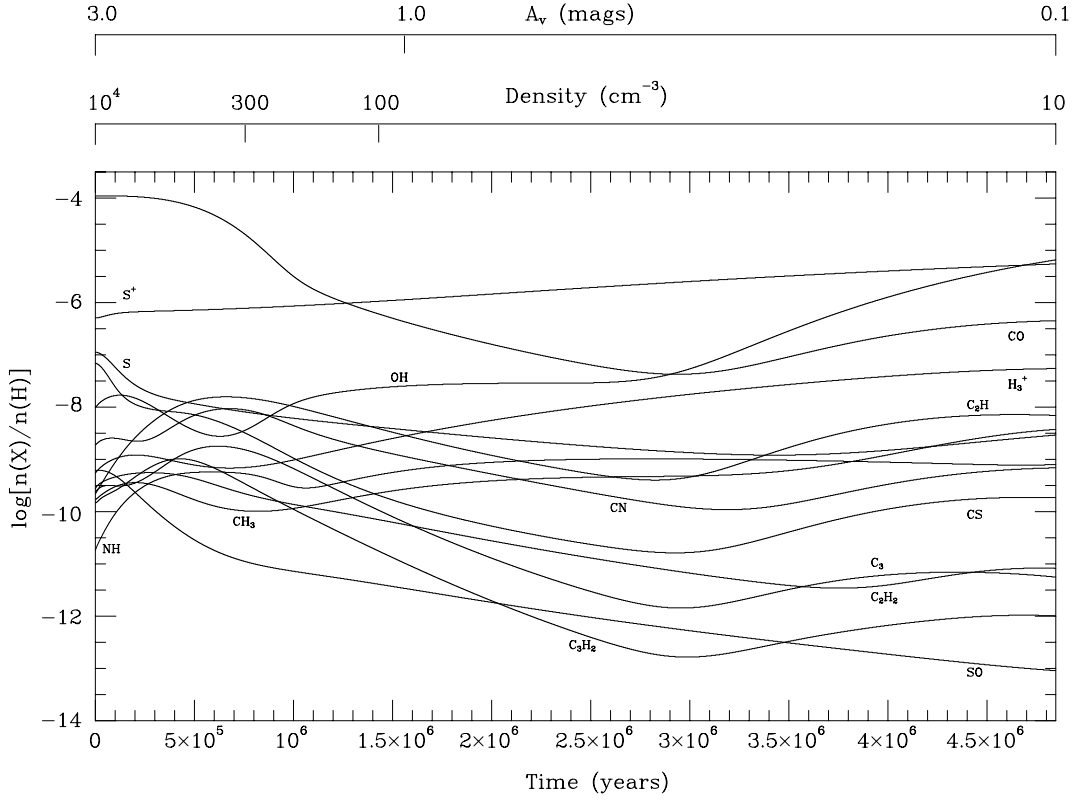


Figure 3. The fractional abundance of a selection of species relative to hydrogen over time, during the expansion phase.

Table 2. Column densities of species at a spatial density of 100 cm^{-3} . Observed column densities for ζ Per have been taken from the literature, where available. Observed column densities enclosed in brackets represent observations made in other lines of sight; some are discussed in the text. The notation a(b) represents a $\times 10^b$.

Species	Observed	Collapse	Expansion
H ₂	3.2(20)–7.1(20) ^a	8.2(+20)	8.5(+20)
S	1.8(13) ^b	8.1(+13)	7.1(+12)
O	–	7.4(+17)	5.3(+17)
C	–	1.7(+16)	8.2(+15)
S ⁺	1.6(16) ^c	2.1(+16)	1.8(+15)
CS	[0.5(12)–2(12)] ^d	8.2(+11)	3.5(+11)
SO	[1.0(12)–1.0(13)] ^d	2.0(+09)	7.0(+09)
CO	6.1(14) ^b	8.7(+14)	1.0(+15)
C ₂ H	[7.0(12)] ^e	1.9(+12)	6.7(+12)
C ₃ H ₂	[4.8(12)] ^e	5.5(+09)	3.1(+10)
NH	1.0(12) ^f	5.0(+10)	8.6(+11)
CN	3.0(12) ^g	4.0(+11)	2.5(+12)
OH	4.0(13) ^g	3.6(+13)	4.0(+13)
H ⁺ ₃	8.0(14) ^h	2.2(+12)	3.8(+12)
C ₃	–	6.4(+10)	1.8(+11)
HCO ⁺	–	1.5(+11)	2.2(+11)
HCN	–	3.7(+09)	6.0(+10)

^aSavage et al. (1977), ^bSnow (1977), ^cSnow, Lamers & Joseph (1987), ^dLucas & Liszt (2002), ^eLucas & Liszt (2000), ^fMeyer & Roth (1991), ^gFelenbok & Roueff (1996), ^hMcCall et al. (2003).

Table 3. Column densities of species at a spatial density of 300 cm^{-3} . Observed column densities for ζ Oph have been taken from the literature, where available. Observed column densities enclosed in brackets represent observations made in other lines of sight; some are discussed in the text. The notation a(b) represents a $\times 10^b$.

Species	Observed	Collapse	Expansion
H ₂	4.6(20) ^a	1.2(+21)	1.2(+21)
S	8.5(13) ^b	2.7(+14)	2.0(+13)
S ⁺	1.2(16) ^b	2.9(+16)	1.9(+15)
O	5.0(17) ^c	1.0(+18)	7.0(+17)
C	2.2(17) ^c	1.9(+17)	9.4(+16)
SO	[1.0(12)–1.0(13)] ^e	4.7(+10)	2.7(+10)
CO	2.2(15) ^a	4.8(+15)	4.9(+16)
C ₂ H	[7.0(12)] ^f	9.8(+12)	3.7(+13)
C ₃ H ₂	[4.8(12)] ^f	1.2(+11)	8.3(+11)
NH	8.8(11) ^g	8.0(+10)	1.3(+12)
CN	2.5(12) ^a	5.0(+12)	2.2(+13)
OH	4.6(13) ^a	1.0(+13)	8.9(+12)
H ⁺ ₃	[3.8(14)] ^h	9.8(+11)	1.7(+12)
C ₃	1.6(12) ⁱ	1.3(+12)	3.7(+12)
HCO ⁺	9.1(11) ^a	2.2(+10)	4.0(+10)
HCN	3.6(11) ^a	1.2(+10)	1.5(+11)
CH	2.5(13) ^a	9.1(+13)	2.4(+14)

^aLiszt & Lucas (2001), ^bMorton (1975), ^cvan Dishoeck (1998), ^dLucas & Liszt (1997), ^eLucas & Liszt (2000), ^fLucas & Liszt (2000), ^gCrawford & Williams (1997), ^hMcCall et al. (1999), ⁱMaier et al. (2001).

In Table 3, we report instead the H₃⁺ column density observed by McCall et al. (1999) towards Cygnus OB2 at a visual extinction of ≈ 10 mag and a density of $\approx 300 \text{ cm}^{-3}$; they derive a column density of $\sim 4 \times 10^{14} \text{ cm}^{-2}$ – over two orders of magnitudes larger than our

theoretical values. Although this latter discrepancy may be caused by the different physical conditions (A_V) between Cygnus OB2 and our models, this does not justify the difference between observed and theoretical column densities for ζ Per in Table 2. This confirms that

H_3^+ is indeed a problem case: note that all diffuse cloud models fail to account for such high values of its abundance. Possible solutions have been offered in terms of a particular spatial distribution of matter (Cecchi-Pestellini & Dalgarno 2000), or in terms of a high cosmic ray ionization rate (McCall et al. 2003). Neither of these approaches is yet validated and we have therefore decided not to implement them in our models. Note that in the expansion phases represented in Tables 2 and 3, a significant fraction of sulphur still remains on the grains. The computed gas-phase S^+ fraction is seen to rise steadily with time in Fig. 3, as sulphur is released from the grains. Finally, we note that our HCN/HNC ratio is inverted if compared to observations: we believe that this may be a result of limitations in the chemical network that we have utilized, as, most probably, the latter lacks many relevant destruction routes for HNC.

We must note that the visual extinction in our models at a density of 300 cm^{-3} is 1.5 mag, somewhat larger than is expected for the cloud in the line of sight to ζ Oph. As a result, our column densities may overestimate their true values somewhat.

4 DISCUSSION

The results of Section 3 show that it is plausible to consider that diffuse clouds may be in a state of expansion or of contraction, rather than in some static configuration (as is frequently assumed). We have not attempted to fit the abundances observed on any particular line of sight; indeed, the simple model used here is incapable of providing such a detailed fit. Clearly, there are discrepancies between some theoretically predicted and observationally determined column densities. Nevertheless, the crude models investigated here do show chemical abundances that have the general chemical characteristics of diffuse clouds. Here, we discuss whether these calculations indicate that there are potential observational tracers of the dynamical state of the gas. While we accept that there are some uncertainties with the approach adopted here, we consider that the *ratio* of abundances in the expansion and collapse cases may be useful in identifying molecular tracers of the dynamical state of the cloud.

We find that the ratios of abundances in the expansion phase relative to those in the contraction phase as a function of density take a wide range of values, and that several species – notably C_2H_2 , CN, SO and CS – are quite sensitive to density (not shown). Thus, if the population of the observed diffuse clouds contains members in states of expansion and others in states of contraction, then we may expect to see wide variations in molecular abundances – as is indeed the case.

Tables 4 and 5 show the column densities, together with their ratios, for all species with a column density of at least $1 \times 10^{10} \text{ cm}^{-2}$ in at least one of the expansion or contraction phases. The ratios in Tables 4 and 5 show wide variation. This variation comes from two sources. First, molecular abundances in the expansion phase are affected significantly by the molecules released from ices by photodesorption. Secondly, atomic ions are more abundant in the contraction phase than in the expansion one because (i) they have not yet depleted and (ii) they recombine relatively slowly, so atomic ions in the collapse phase (which has initially a purely atomic state) tend to be more abundant than in the expansion phase (which is initially largely molecular).

The model collapse and expansion speeds of the cloud may both be changed. Reducing the expansion speed causes the abundance of each molecule to decrease in the expansion phase and results in a decrease of the fractions listed in Tables 4 and 5 (by $\lesssim 30$ per cent for α between 1.0 and 0.2). In the case of the atoms/ions,

Table 4. Column densities of species in the collapse and expansion phases at a density of 100 cm^{-3} . The ratio between these column densities is also listed for each species. Only those species which have a column density in excess of $1 \times 10^{10} \text{ cm}^{-2}$ in either the collapse or expansion phases and a ratio in excess of 10 (or less than 0.1) are listed. The notation a(b) represents $a \times 10^b$.

Species	Column Density		Ratio (E/C)
	Collapse	Expansion	
NH	5.0(+10)	8.6(+11)	1.7(+01)
NH ₂	1.8(+10)	7.1(+11)	3.9(+01)
CH ₄	6.5(+05)	3.0(+12)	4.6(+06)
NH ₃	7.3(+07)	5.1(+11)	7.0(+03)
HNO	1.8(+09)	5.1(+10)	2.8(+01)
HNC	4.4(+09)	1.7(+11)	3.8(+01)
HCN	3.7(+09)	6.0(+10)	1.6(+01)
H ₂ S	3.1(+07)	2.0(+11)	6.3(+03)
C ₂ H ₂	1.3(+09)	1.2(+11)	9.5(+01)
Si	1.2(+10)	4.1(+08)	3.3(−02)
S	8.1(+13)	7.1(+12)	8.7(−02)
Na	1.5(+12)	8.3(+10)	5.4(−02)
Mg	6.0(+10)	3.3(+09)	5.5(−02)
Na ⁺	3.1(+14)	1.0(+13)	3.4(−02)
Mg ⁺	1.1(+13)	4.9(+11)	4.4(−02)
Si ⁺	1.1(+13)	3.9(+11)	3.6(−02)
S ⁺	2.1(+16)	1.8(+15)	8.6(−02)
Fe ⁺	3.1(+12)	1.1(+11)	3.5(−02)

Table 5. Column densities of species in the collapse and expansion phases at a density of 300 cm^{-3} . The ratio between these column densities is also listed for each species. Only those species which have a column density in excess of $1 \times 10^{10} \text{ cm}^{-2}$ in either the collapse or expansion phases and a ratio in excess of 10 (or less than 0.1) are listed. The notation a(b) represents $a \times 10^b$.

Species	Column Density		Fraction (E/C)
	Collapse	Expansion	
NH	8.0(+10)	1.3(+12)	1.6(+01)
NH ₂	3.8(+10)	8.2(+11)	2.2(+01)
CH ₄	5.2(+07)	2.6(+12)	4.9(+04)
NH ₃	2.0(+08)	4.3(+11)	2.2(+03)
CO	4.8(+15)	4.9(+16)	1.0(+01)
HNC	1.2(+10)	2.9(+11)	2.4(+01)
HCN	1.2(+10)	1.5(+11)	1.3(+01)
HNO	1.1(+10)	1.8(+11)	1.6(+01)
H ₂ CN	3.5(+08)	1.3(+10)	3.9(+01)
H ₂ S	2.7(+08)	2.1(+11)	7.9(+02)
C ₂ H ₂	4.4(+10)	5.3(+11)	1.2(+01)
N ₂	6.9(+13)	3.9(+15)	5.7(+01)
PN	8.6(+08)	4.1(+10)	4.8(+01)
C ₅ H	2.3(+09)	3.3(+10)	1.4(+01)
C ₆	1.1(+10)	1.7(+11)	1.6(+01)
C ₆ H	3.7(+09)	1.1(+11)	2.9(+01)
C ₇	1.4(+09)	3.9(+10)	2.7(+01)
Si	6.9(+10)	8.2(+08)	1.2(−02)
S	2.7(+14)	2.0(+13)	7.2(−02)
Na	4.2(+12)	5.4(+10)	1.3(−02)
Mg	2.1(+11)	4.7(+09)	2.2(−02)
Fe	2.2(+10)	2.9(+08)	1.3(−02)
Na ⁺	4.1(+14)	4.3(+12)	1.0(−02)
Mg ⁺	1.5(+13)	3.3(+11)	2.2(−02)
Si ⁺	1.5(+13)	1.9(+11)	1.3(−02)
S ⁺	2.9(+16)	1.9(+15)	6.7(−02)
Fe ⁺	4.2(+12)	4.9(+10)	1.2(−02)

their abundances are increased in the expansion phase, resulting in a subsequent increase in the relevant fractions (by ≈ 30 to 340 per cent for α between 1.0 and 0.2). Thus, if the expansion were to be governed by the sound speed, the fractions listed in Tables 4 and 5 would be somewhat larger for the molecules, but smaller for the atoms/ions. Retarding the collapse speed, on the other hand, tends to cause the abundance of the molecules and of the atoms/ions to decrease and increase in the collapse phase, respectively. In turn, this results in increases in the molecule fractions (by $\lesssim 30$ per cent for $B = 1.0$ to 0.6; the exception being PN, which experiences a reduction of 36 per cent) and reductions in the atom/ion fractions (by $\lesssim 40$ per cent for $B = 1.0$ to 0.6; the exception being Na, which experiences an increase of 18 per cent) listed in Tables 4 and 5.

We find that increasing the photoevaporation rate during the expansion phase increases the abundance of all the species, owing to the increased injection of mantles into the gas phase. Computations for many parameter variations (not presented here) show that reducing the expansion speed results in larger fractions for all species listed in Tables 4 and 5.

We conclude that strong signatures in the diffuse interstellar gas should exist in interstellar clouds, if the population of diffuse clouds contains some members in contraction and some in expansion, as envisaged here. Simple hydrides and hydrocarbons should be more abundant in the expansion phase, whereas atomic ions should be more abundant in the collapse phase. In this picture, the chances of observing the 100 and 300 cm^{-3} stages of the cloud evolution are reasonable, if one assumes that the envisaged structures are very common and, indeed, everywhere in the cloud. We note, however, that beam confusion may be a problem in the case where members of both populations are present within the same cloud and along the same line of sight.

ACKNOWLEDGMENTS

The authors are grateful to the referee for very useful suggestions that improved on a previous version of this paper. RJP thanks PPARC for financial support of his work. SV thanks the Italian Space Agency (ASI) for financial support.

REFERENCES

- Bachiller R., 1996, *ARA&A*, 34, 111
 Cecchi-Pestellini C., Dalgarno A., 2000, *MNRAS*, 313, L6
 Crawford I. A., Williams D. A., 1997, *MNRAS*, 291, L53
 Dyson J., Williams D. A., 1997, *The Physics of the Interstellar Medium*. Institute of Physics Publishing, Bristol
 Federman S. R., Allen M., 1991, *ApJ*, 375, 157
 Felenbok P., Roueff E., 1996, *ApJ*, 465
 Goldsmith P. F., Langer W. D., Wilson R. W., 1986, *ApJ*, 303, L11
 Habing H. J., 1968, *Bull. Astron. Inst. Netherlands*, 19, 421
 Hartquist T. H., Falle S. A. E. G., Williams D. A., 2003, *Ap&SS*, in press
 Hollenbach D. J., Chu S.-I., McCray R., 1976, *ApJ*, 208, 458
 Jones A. P., Williams D. A., 1984, *MNRAS*, 209, 955
 Liszt H. S., Lucas R., 2001, *A&A*, 370, 576
 Lucas R., Liszt H. S., 1997, in van Dishoeck E. F., ed., *Proc. IAU Symp.* 178, *Molecules in Astrophysics: Probes and Processes*. Kluwer, Dordrecht, p. 421
 Lucas R., Liszt H. S., 2000, *A&A*, 358, 1069
 Lucas R., Liszt H. S., 2002, *A&A*, 384, 1054
 McCall B. J., Geballe T. R., Hinkle K. H., Oka T., 1999, *ApJ*, 510, 251
 McCall B. J. et al., 2003, *Nat*, 422, 500
 Maier J. P., Lakin N. M., Walker G. A. H., Bohlender, D. A., 2001, *ApJ*, 553, 267
 Meyer D. M., Roth K. C., 1991, *ApJ*, 376, L49
 Millar T., Farquhar P., Willacy K., 1997, *A&AS*, 121, 139
 Morton D. C., 1975, *ApJ*, 197, 85
 Nejad L. A. M., Williams D. A., Charnley S. B., 1990, *MNRAS*, 246, 183
 O’neill P. T., Williams D. A., 1999, *Ap&SS*, 266, 539
 O’neill P. T., Viti S., Williams D. A., 2002, *A&A*, 388, 346
 Price R. J., Crawford I. A., Barlow M. J., 2000, *MNRAS*, 312, L43
 Rawlings J. M. C., Hartquist T. W., Menten K. M., Williams D. A., 1992, *MNRAS*, 255, 471
 Savage B. D., Drake J. F., Budich W., Bohlin R., 1977, *ApJ*, 216
 Snow T. P., 1977, *ApJ*, 216, 724
 Snow T. P., Lamers H. J. G. L. M., Joseph C. L., 1987, *ApJ*, 321, 952
 Spitzer L., 1978, *Physical processes in the interstellar medium*. Wiley-Interscience, New York, p. 333
 van Dishoeck E. F., 1998, in Hartquist T. W., Williams D., eds, *The Molecular Astrophysics of Stars and Galaxies*. Clarendon Press, Oxford, p. 53
 van Dishoeck E. F., Black J. H., 1988, *ApJ*, 334, 771
 Wagenblast R., 1992, *MNRAS*, 259, 155
 Wagenblast R., Williams D. A., 1993, in Millar T. J., Williams D. A., eds, *Dust and Chemistry in Astronomy*. Institute of Physics Publishing, Bristol
 Westley M. S., Baragiola R. A., Johnson R. E., Baratta G. A., 1995, *Planet. Space Sci.*, 43, 1311

This paper has been typeset from a $\text{\TeX}/\text{\LaTeX}$ file prepared by the author.